



**UNI BCCS
TECHNICAL REPORT SERIES**

**Numerical modelling of organic waste dispersion
from marine fish farms with consideration to
topography variations**

**Alfatih Ali, Øyvind Thiem,
and Jarle Berntsen**

REPORT No. 28

October 28, 2010

*Deliverance to the Research Council of Norway through the project
"Ecosystem Responds to Aquaculture Induced Stress" (ECORAIS).
Contract number 190474/s40*

UNI Research
the University of Bergen research company

BERGEN, NORWAY

BCCS Technical Report Series is available at <http://www.bccs.uni.no/publications/>

Requests for paper copies of this report can be sent to:

Bergen Center for Computational Science, Høyteknologisenteret,
Thormøhlensgate 55, N-5008 Bergen, Norway

Abstract

In this study, a three-dimensional particle tracking routine coupled to a terrain following ocean model is used to investigate the dispersion and the deposition of fish farm particulate matter like uneaten food and fish faeces on the seabed. The particle tracking model uses the computed local flow field for advection of the particles and random movement to simulate the turbulent diffusion. Each particle is given a settling velocity which may be drawn from a normal distribution according to sinking velocity measurements of faecal and feed pellets.

Considering the tidal currents as the only driving forces, the results show that the maximum concentration of organic waste for the fast sinking particles is found under the fish cage and continue decreasing away from the cage area. The maximum can split into two maximum peaks located at both sides in the current direction outside the fish cage area, leaving the area below the cage less polluted. This process very much depends on the sinking time (time needed for a particle to settle at the bottom), the tidal velocity, and the fish cage size.

If the sinking time is close to a multiple of the tidal period (small and very slow-sinking particles), the maximum concentration point will end up under the fish cage. This is due to the nature of the tidal current first advecting the particles away and then bringing them back when the tide reverses. This is independent on the current strength. Increasing the cage size increases the likelihood that the maximum waste accumulation ends up beneath the fish farm, and larger farms usually means larger biomasses which can make the local pollution even more severe.

Features of the deposition footprint such as its shape/size, and the maximum accumulation due to variations in bottom topography are also investigated. The results show that for slight variation in bathymetry, there will be no significant affects on the particles distribution for sites with weak currents. However, the difference will be more prominent when the tide is stronger since topographic turbulence then affects the flow pattern.

The model is validated by using an analytical model, which uses an exact harmonic representation of the tidal currents, and the results show an excellent agreement.

Contents

1	Introduction	3
2	The coupled model	4
2.1	The Bergen Ocean Model	4
2.2	The Particle tracking routine	5
2.2.1	Settling velocity	5
2.3	Simulation results	6
3	The analytical model	9
3.1	Model description	9
3.2	Results	10
3.2.1	Periodic distribution	10
3.2.2	One or two maximum concentration regions	12
4	The coupled model in a fjord with one opened boundary	14
4.1	Model setup	14
4.2	Results	14
5	Sensitivity to bottom topography	17
5.1	Setup	17
5.2	Results	19
6	Summary	23

1 Introduction

Fish farming is a rapid growing industry and the trade in seafood is the second largest export industry in Norway after oil and gas. Globally, the fish farming supplies more than 50 percent of the fish consumed by human. Due to its high profits, it has become a major attractive market for investors. Therefore the fish farming industry may contribute to reducing the pressure on the natural fish resources.

However, the potential negative impacts due to spreading of diseases and fish louses between the farmed and wild stocks is a major concern. A large part of the Norwegian wild salmon stocks has now become extinct, and it is questioned if the fish farming in the fjords is the reason. The organic waste from fish farming and its effect on the marine ecosystem has lately also made fish farms front-page news. Silvert and Sowles [1996] summarized the major sources of the environmental impact in the vicinity of fish farms. The focus was on dispersion and deposition of the organic matter, mainly fish faeces and uneaten food, where physical and biological effects and the structure of the fish cage were taken into account.

Modelling waste dispersion and deposition is considered as the most cost-effective tool for estimating the environmental impact of the fish farming industry. However, good aquaculture modelling which provides tools to understand, assess, predict, and managing this impact is still immature and needed. In particular the goal is develop numerical model tools to answer question like where the highest concentration of the organic waste will be located and why, and what is the magnitude of the of its impact on the marine ecosystem and benthic habitats?

Hydrodynamic models coupled to particle tracking models are used to study the dispersion of fish farm waste in some studies such as Panchang et al. [1997], Dudley et al. [2000], and Doglioli et al. [2004]. However, in most of these studies, only two-dimensional depth averaged versions of the the hydrodynamic models are considered. In Doglioli et al. [2004], for instance the vertically averaged flow is computed by the two-dimensional Princeton Ocean Model and then used to derive a three-dimensional flow field. Since it is important to account for change in bathymetry and the vertical exchange of water masses, the 3D modelling is necessary.

In this work, a three-dimensional particle tracking routine nested into the three-dimensional hydrodynamical σ -coordinate Bergen Ocean Model (BOM) is used to simulate the dispersion of organic waste from a single cage. BOM uses a mode split technique for the sake of computation efficiency. The parallel version of BOM allows for large model domain with fine grid. The particle tracking model uses the modeled tidal current velocity field for advection of particles and random movement to simulate turbulent diffusion. Each particle is given a settling velocity which may be drawn from a normal distribution according to sinking velocity measurements of faecal and feed pellets such as in Cromey et al. [2002].

The results show that when the tide is the only driving force, the maximum concentration area of organic waste depends on the mean sinking time (the time required for a particle to sink through the water column and settle at the bottom), the tidal velocity strength, and the fish cage size. The area with highest concentration of particles can be as one peak (under the cage) or as two peaks, one located on each side of the fish cage.

The maximum accumulation area is found beneath the cage for fast sinking particles and for particles where the sinking time is close to a multiple of tidal periods. It is worth noticing that for the last type of particles the maximum concentration point will be located under the fish cage independent of the strength of the tide due to the nature of the tidal currents reversing its direction after around six hour. Particles with sinking times that does not fall under the two categories above will distribute into two maximum peaks. Increasing cage size increases the likelihood for that food and faecal pellets will have a maximum concentration beneath the fish farm. Larger farms also means larger biomasses which makes it even more likely that the pollution will be more severe.

Features of the deposition footprint such as its shape/size, and the maximum accumu-

lation due to variations in bottom topography are also investigated.

The results are validated by comparing the model with a simple analytical model which uses an exact harmonic representation of the tidal current, an excellent agreement is achieved.

The report is organized as follows. The model tool is presented in Section 2, which contain a description of BOM together with the particle tracking model and its integration with the ocean model. A section of an idealized fjord is used to investigate the particle accumulation at the seabed and its sensitivity to the settling velocity are shown. The simple analytical model is presented in Section 3, and used to validate the model results in Section 2. Further a bay setup is presented in Section 4. In Section 5, sensitivity to small variation in bottom topographies around the fish cage area and its affect on the particles accumulation is studied. This is slightly similar to a previous study by Jusup et al. [2007], but in that study no a hydrodynamic model was used. In the last section a summary of the overall study is presented.

2 The coupled model

In this section, a description of the Bergen Ocean Model (BOM) and the particle tracking model that uses the Lagrangian approach is given. The full model system is denoted as the coupled model.

2.1 The Bergen Ocean Model

Bergen Ocean Model is a terrain-following three-dimensional hydrodynamical numerical ocean model which utilizes the σ -coordinate in the vertical direction given by the mapping $\sigma = \frac{z-\eta}{H+\eta}$. Here z is the vertical coordinate, η is the surface elevation and H is the bottom depth. The model uses the mode splitting technique which separates the governing equation into external depth averaged mode for simulating the fast moving surface gravity waves, and internal mode to model the slow moving internal gravity waves, see for example Berntsen et al. [1981] and Kowalik and Murty [1993].

Nonhydrostatics pressure capabilities have been implemented enabling the model to simulate small-scale physical processes with grid resolution less than one meter (laboratory experiment Berntsen et al. [2006]). The model uses a finite difference method to solve the governing equations, namely the momentum, conservation and continuity equations, with a C-grid discretization technique. The mathematical variables are the velocity field components, density, pressure, temperature and salinity. BOM is implemented in Fortran 90 code and is freely available at <http://www.mi.uib.no/BOM/>.

The tide is used as driving force. The model domain is an idealize fjord of 4 km length, 1.2 km width and constant depth of 100 m, which coinciding with x, y , and z axes, respectively (Figure 1). The horizontal grid resolution is $\Delta x = \Delta y = 100$ m and 21 equidistant σ – coordinate layers are used in the vertical. The horizontal dimension of the fish cage is 50×50 m², centered at the grid cell at (2000, 600). The particles are released randomly within the cage at 5 m depth. The western and the eastern boundaries are open and here seven grid cells wide flow relaxation zones are used. In the flow relaxation zones, the water elevation is updated at each time step according to

$$\phi = (1 - \alpha) \cdot \phi_{int} + \alpha \cdot \phi_{ext}, \quad (1)$$

where ϕ_{int} contains the unrelaxed values computed by the model and ϕ_{ext} is specified external value. The relaxation parameter α varies smoothly from from 1 at the open boundary to 0 at the innermost cell of the boundary zone. This method is called Flow Relaxation Scheme (FRS) and described in Martinsen and Engedahl [1987]. The tidal surface elevation in both FRS zones is equal and given by the form

$$\eta(t) = \eta_0 \cdot \cos(\omega \cdot t - \theta). \quad (2)$$

Here η_0 denotes the tidal elevation amplitude, $\omega = \frac{360}{T}$ is the tidal frequency where T is the tidal period, and θ is the tidal phase. The approximated tidal flow is therefore in the x direction along west-east, and has a similar cosine signal with the same frequency and phase as in Eq. (2). No variations in the water density is accounted for and also the fish cage has no effect on the water flow. The model is run until all particles have settled on the seabed. The tidal period is $T = 12.4206$ hours and phase is $\theta = 90$.

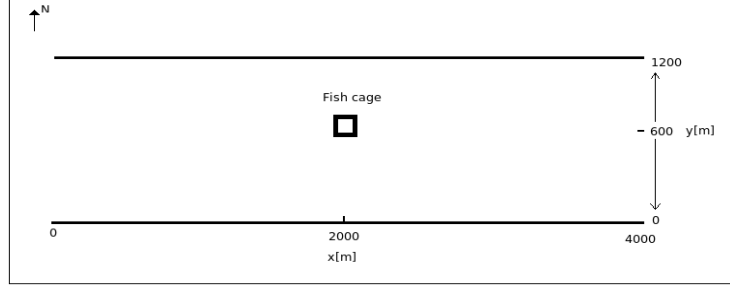


Figure 1: Horizontal configuration of the model domain (Idealized Fjord).

2.2 The Particle tracking routine

The particle tracking model, which has been used in Thiem et al. [2008], accounts for three processes that influence the particle movement. Advection by current velocity field, random diffusion due to turbulence, and vertical movement towards the sea bed (sinking) caused by particles weights. The particle position $\vec{x}(t) = (x(t), y(t), z(t))$ at the time step $t_n = (t + n * \Delta t)$, can then be given by :

$$\vec{x}(t_n) = \vec{x}(t_{n-1}) + \vec{U}(t_{n-1}) * \Delta t + r * \vec{U}_{std}(t) * \Delta t - (0, 0, w_s) * \Delta t, \quad (3)$$

where $\vec{U}(t) = (U(t), V(t), W(t))$ is the current velocity field in (x, y, z) -direction, $\vec{U}_{std}(t)$ denotes the standard deviation of \vec{U} , w_s is the particle settling velocity, and r is a Gaussian distributed stochastic variable with mean = 0 and standard deviation = 1. The Fortran function *random_number* is used to generate a uniformly distributed random number in $[0, 1]$ combined with Box-Muller transform to convert into the Gaussian distribution.

The particle tracking model is integrated with the ocean model so that the approximated local flow field from the ocean model is used to propagate the particles at each time step. This is computationally demanding, however, in high resolution studies where the flow field are constantly changing this can be necessary.

Particles that hit the bottom is considered as settled and taken out of the simulation. The particles accumulation at the bottom is computed by counting the particles that hit the bottom within grid cells of $5 \times 5 \text{ m}^2$ size. Figure 2 shows how the particle model cycle is nested into the ocean model cycle.

2.2.1 Settling velocity

The horizontal distance particles travel depends on the sinking time given by the settling velocity and the bottom depth, and the local current. The settling velocity of particles varies due its physical and biological characteristic such as its size, weight, density, absorption, digestibility and its components nature. Fish size and fish type are also important for the

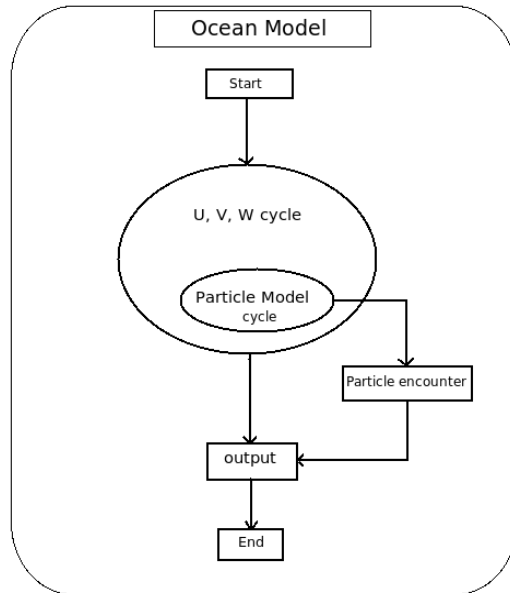


Figure 2: The flow chart shows the integration of the particle tracking model with the ocean model, and U , V , and W represent the velocity components estimated by the ocean model.

settling velocity measurement of faecal pellets. For example Cromey et al. [2002] conducted measurement experiments of the settling velocity for the Atlantic salmon (3.39 kg) fish faeces. Sediment traps were used under the cage for faeces collection and then immediately transferred to a glass cylinder for testing. They found that the settling velocity is normally distributed with mean $\mu = 0.032$ m/s and standard deviation $\sigma = 0.011$ m/s. For small faecal pellets of size 0.3 – 2.5 mm of the sea bream (*Sparus aurata*), Magill et al. [2006] measured settling velocity of 0.0048 m/s. When it comes to the settling of food pellets, Chen et al. [1999] found a mean settling velocity of 0.128 m/s. These values are used in the numerical simulations in Figure 15. In lack of better parameters for mean settling velocity and the standard deviation this study will focus on the parameters given in Cromey et al. [2002], Magill et al. [2006] and Chen et al. [1999].

2.3 Simulation results

In this part, we investigate how the settling velocity affects the particle distributions over a flat bottom. The initial horizontal position for each particle is chosen randomly with uniform distribution.

Figure 3 shows the particles accumulations at the bottom computed for different means and standard deviations of the settling velocity as variations in particle characteristics are considered. 1.62×10^5 particles are released continuously over two tidal cycles. The tidal elevation amplitude at the open boundaries is 0.25 m/s which is resulted in 0.25 m/s tidal velocity amplitude.

The initial vertical depth for particles is 5 m, therefore the falling length is 95 m.

Accordingly, the results in Figure 3 could be clarified and classified as follows:

1. Particles with mean settling velocity of 0.128 m/s, its mean sinking time approximately 12 minutes, has one maximum (peak), (black line Figure 3). These particles sink very fast that the influence of the horizontal current is marginal.
2. For particles with mean settling velocities in the range 0.032 to 0.048 m/s (solid

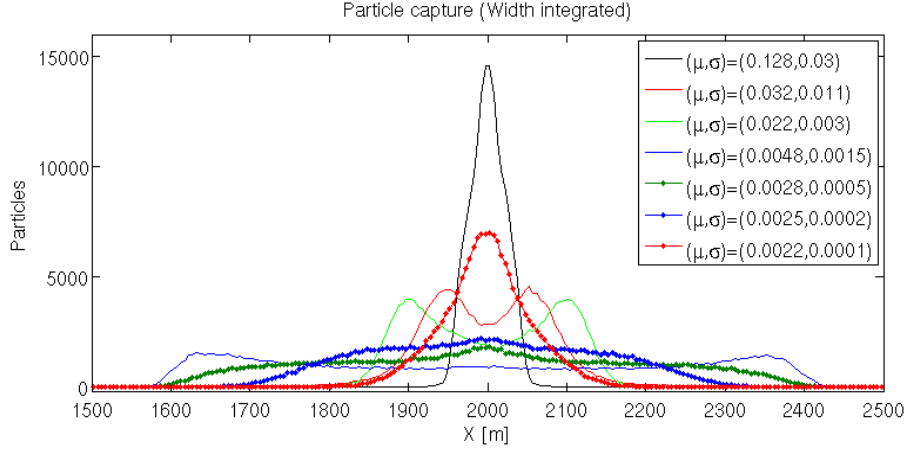


Figure 3: Number of particles settled (width integrated). μ and σ are the mean and standard deviation of the settling velocity, respectively. No random movement. The tidal velocity amplitude is 0.025 m/s. The cage center is at $x = 2000$ m.

lines, Figure 3), the maximum is split into two peaks away from the cage centre. This splitting is due to the mean sinking time (0.8 to 5.5 hours) approaching $T/2$. Which means that most of the particles will spend longer time in the water column, therefore they will be dispersed in one direction and settled before the half of the tidal cycle.

3. For particles with mean settling velocities in the range 0.0028 to 0.0022 m/s (dot-solid lines, Figure 3), the two peaks emerge into one peak beneath the cage centre. This is due to the mean sinking time (9.4 to 11.99 hours) approaching the full tidal cycle. Meaning that most of the particles will disperse and return as the tide reverses. More over, they can settle at the same x-location as they were released if the sinking time is equal to a multiple of the full tidal cycle. Here, the settling velocities are one order much less than the horizontal velocity, which means that the influence of the horizontal current is very high. However when the mean sinking time is quite long, most particles may disperse and then return to settle closer to the fish cage.

This means, in tidal driven areas the particles will be sorted according to the current velocity, depth, and weight. If the mean sinking time is close to the full tidal cycle, then the particles will accumulate mainly under the fish cage. Particles with sinking times approaching the half of the tidal cycle will have the widest possible spreading from the fish cage with less concentration beneath the cage, see the blue-solid curve in Figure 3.

This particle footprint is obviously due to the nature of the tidal current and will be explained in more details in the next section using the analytical model. Figure 4 shows paths of some particles for some cases shown in Figure 3 with zero standard deviation for each run.

In the particle tracking routine, the random diffusion is computed from variations in the flow field using the sample standard deviation

$$\vec{U}_{std} = \sqrt{\frac{\sum_{i=1}^N (\vec{U}_i - \vec{\bar{U}})^2}{N - 1}}, \quad (4)$$

where N is the number of the velocity points, $\vec{\bar{U}}$ is the mean of the velocity field \vec{U}_i and i is the index over the velocity points. In the present model setup and forcing, the variations

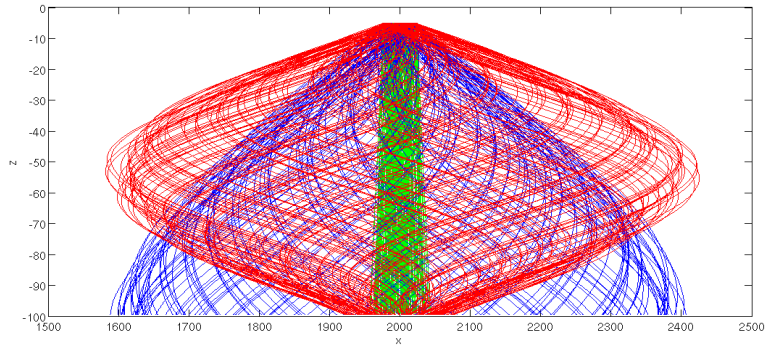


Figure 4: Particle paths, for green: $\mu = 0.128$ m/s, blue curves: $\mu = 0.0048$ m/s, and red: $\mu = 0.0022$ m/s.. $\sigma = 0$. releasing time $T = 24$ h. The tidal velocity amplitude is 0.025 m/s.

in the velocity is very small due to the simplicity of the model domain (flat bottom and no density variations). This means that the random diffusion has small effects on the particles distribution at the sea bottom, see Fig. 5. There are other ways to implement the random diffusion like using a constant diffusion parameter which would lead to more random variations in the particle distribution, but using Eq. (4) is a simple check that the particle tracking routine works satisfactory. The particle tracking experiments to be presented later are run without random diffusion.

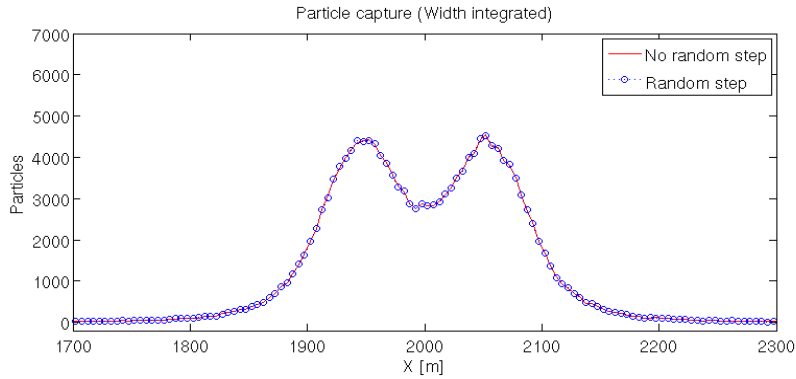


Figure 5: Random step (circles) vs no random (red curve) step with $\mu = 0.032$, $\sigma = 0.011$ m/s. The tidal velocity amplitude is 0.025 m/s.

3 The analytical model

The simple model setup and forcing used for the coupled model in Section 2 open for validation through using a two-dimensional (x, z) analytical model. In this section a description of the analytical model and its comparison with the coupled model is presented. The sensitivity of the particle distribution to the settling velocity, water depth, tidal velocity, and cage size is investigated.

3.1 Model description

The current flow field estimated by the ocean model in Section 2 is a barotropic tidal flow along the x direction. An exact harmonic representation of the flow field is used to simulate the velocity in x direction, which is given by

$$u(t) = u_0 \cos(\omega * t - \theta). \quad (5)$$

Where u_0 denotes the tidal velocity amplitude. The solution is shown in Figure 6 as an example.

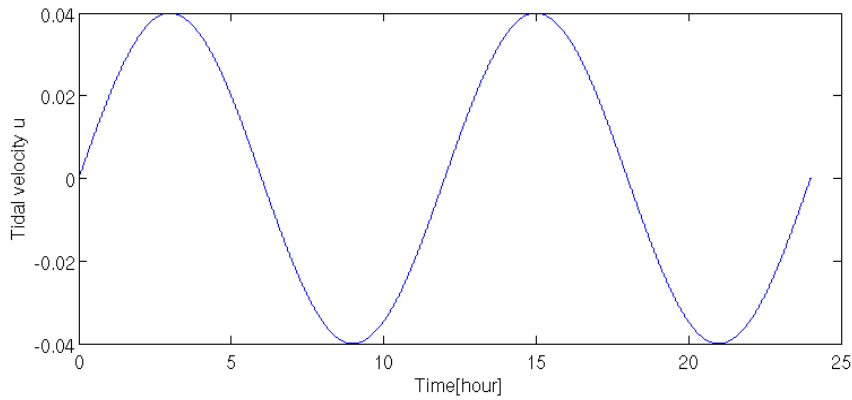


Figure 6: Harmonic representation of the tidal velocity, with amplitude $u_0 = 0.04$ m/s, $T = 12$ hours and phase $\theta = 90$.

The particle position (x, z) at each time step can then be obtained by

$$\begin{aligned} x(t + \Delta t) &= x(t) + u(t) * \Delta t \\ z(t + \Delta t) &= z(t) - w_s * \Delta t, \end{aligned} \quad (6)$$

where w_s is the sinking velocity and Δt is the time step. The particle horizontal location at the bottom is then given by

$$x(t_s) = a + q * (a - b) + \int_{t_0}^{t_0+t_s} u(t) dt. \quad (7)$$

Here t_0 represents the initial time at which the particle is released, t_s is the sinking time which is computed as $\frac{H}{w_s}$, q is a random number uniformly distributed between 0 and 1, and the cage length is represented by an interval $[a, b]$ in which the particle initial position is chosen randomly. For convenience the same sinking time is used for the all particles. This means that no variation in the particle size is taken into account.

3.2 Results

Figure 7 shows that both the analytical and the coupled models produce corresponding particles distribution at the bottom. The settling velocity is 0.032 m/s, (fish faeces).

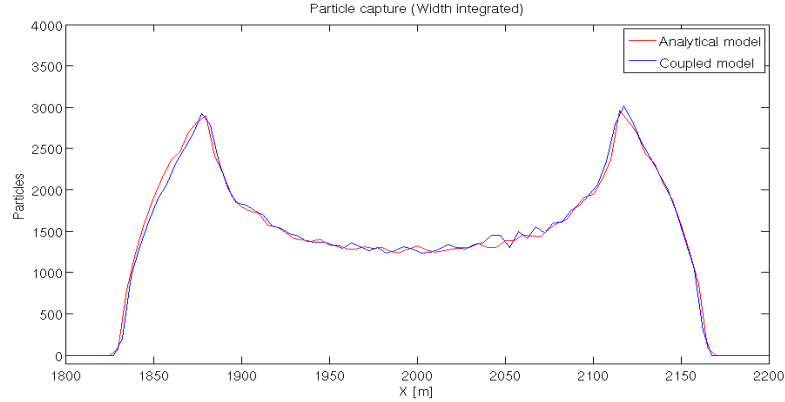


Figure 7: Particles accumulation at the bottom. The coupled model (width integrated) (blue curve) vs the analytical model (red curve). The particles settling velocity is $w_s = 0.032$ m/s, 1.1178×10^5 particles have been released for two tidal cycles, where the tidal velocity amplitude is $u_0 = 0.048$ m/s at the cage center. Cage limits are $(a, b) = (1975, 2025)$, and the vertical depth $H = 95$ m.

3.2.1 Periodic distribution

The particles trajectories for different sinking times are shown in Figure 8. For short sinking times (0.25 hour) the particles settle and accumulate just under the fish cage (solid-blue lines). As the sinking time increases, the particles spread away from the cage center until the sinking time approaches a half of the tidal period ($T/2$). This represents the time at which particles can settle at the maximum possible horizontal distance from the cage center (green lines). Particles that have longer sinking time than half of the tidal period but less than the full tidal period, will start returning as the tide reverses. When the sinking time reaches the full tidal period, all particles will settle under fish cage exactly in horizontal positions at the bottom coinciding with the initial horizontal positions at which they were released.

The accumulation on the seabed is therefore a periodic process with a period equals to the tidal period T . Notice Figure 9 shows that the distribution for particles with sinking time $t_s = 0.025$ hour corresponds exactly to the distribution for particles with sinking time $t_s = (0.025 + T)$ hours.

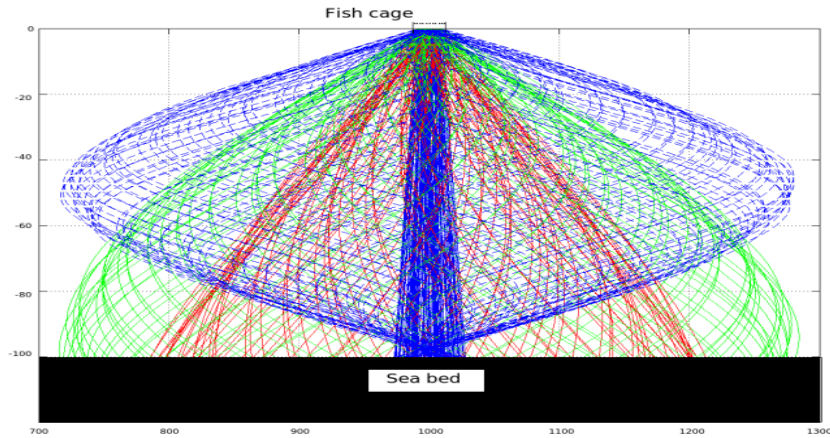


Figure 8: Particle path lines for four different sinking times with tidal amplitude $u_0 = 0.017$ m/s. The sinking times are: 0.25 hour (solid-blue lines), $(0.25 + T/4)$ hours (red lines), $(0.25 + T/2)$ hours (green lines), and $(0.25 + T)$ hours (dashed blue lines). The cage size $b - a = 20$ m.

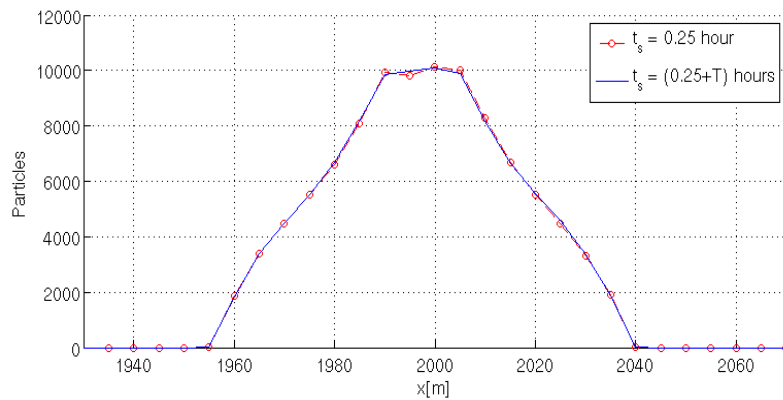


Figure 9: The footprint of particles that have sinking time 0.025 hour and $(0.025+T)$ hours. The falling depth is $H = 100$ m, and the cage size is $b - a = 50$ m. The cage is centered at $x = 1000$, and the tidal velocity amplitude is $u_0 = 0.017$ m/s.

3.2.2 One or two maximum concentration regions

In the previous section it was showed that different settling velocities would lead to one maximum concentration point under the cage center or splits into two maximum regions away from the fish cage. Since sinking times (H/w_s) equal to or longer than the full tidal period will replicate the particles distribution, the focus will be on shorter sinking times than the tidal period. The cage is centered at $x = 1000$, and 10^5 particles are released. The relation between the cage size ($b - a$) and the maximum dispersion distance

$$d_{max}(H, w_s, u_0) = \max \left\{ \int_{t_0}^{t_0 + \frac{H}{w_s}} u_0 \cos(\omega * t - \theta) dt \right\} \quad (8)$$

plays a key role in this process.

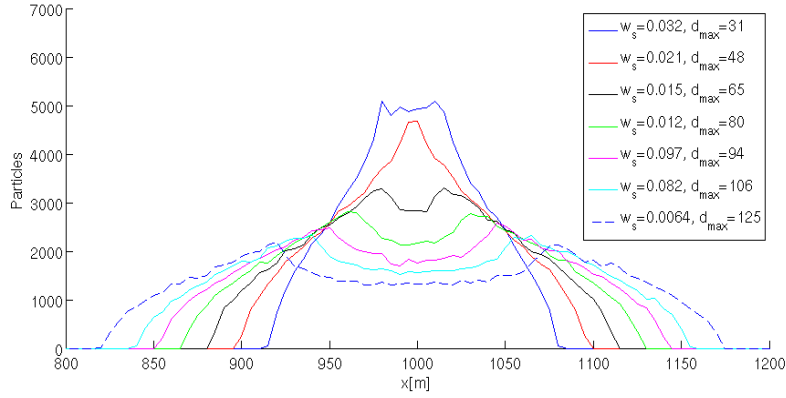


Figure 10: Particle accumulation for different settling velocities w_s . The tidal velocity amplitude is $u_0 = 0.01$ m/s, and falling depth is $H = 100$ m. The cage size is $b - a = 100$ m.

Figure 10 shows that decreasing the settling velocity from 0.032 m/s to 0.0064 m/s will increase d_{max} and when $d_{max} > \frac{(b-a)}{2} = 50$ m, the single maximum starts to split into two maximum peaks away from the cage centre.

The same splitting occurs when the tidal velocity amplitude u_0 is increased from 0.002 to 0.035 m/s, see Figure 11. When $d_{max} > \frac{(b-a)}{2} = 50$ m, the single peak splits into two.

Increasing the water depth will also lead to splitting since the water depth changes the sinking time. In Figure 12, the depth is varied between 20 and 100 m and when $d_{max} > \frac{b-a}{2} = 50$ m the splitting occurs.

The results show that the pollution beneath fish farms will depend on the settling velocity, the tidal currents, and the water depth, which is what should be expected. This means that for a given location the local pollution can depend on the fish species, sizes, and the fish feed, since the sinking velocity depends on these parameters too.

The sensitivity to the cage size ($b - a$) is shown in Figure 13. When $(b - a) = 100$ m or 80 m there will be only maximum under the cage, but when $b - a = 60$ m and smaller, the maximum will start to split into two maximum regions. This is as a result of $d_{max} = 35.98$ m $> \frac{b-a}{2}$. When the cage size is equal to 0 m, it means that particles released from a point source.

Figure 13 shows that using bigger fish cages (which will of course cover bigger areas) to increase production can result in maximum concentration of waste beneath the fish cage in an area that for a smaller fish cage would disperse the waste away from the fish farm.

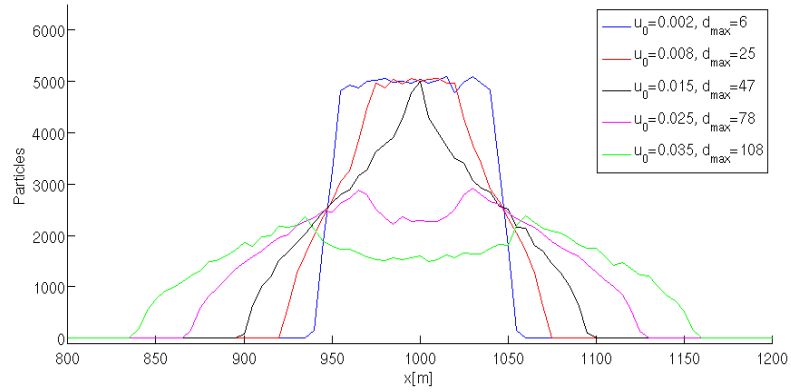


Figure 11: Particles accumulation at the sea bottom for different tidal velocity amplitudes u_0 . The depth is $H = 100$ m, the cage size is $b - a = 100$ m, and the settling velocity is $w_s = 0.032$ m/s.

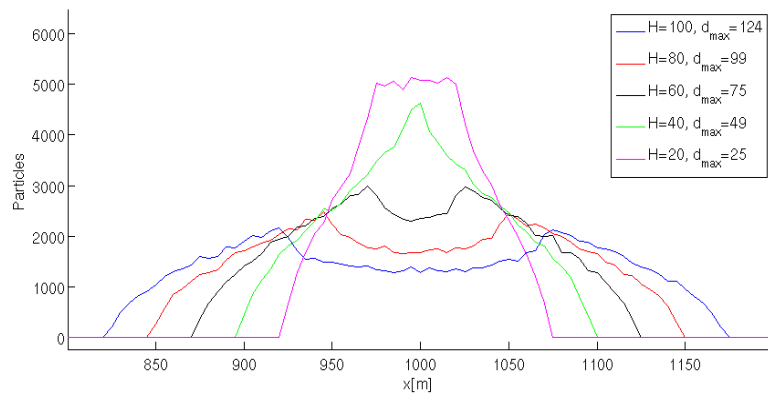


Figure 12: Particles accumulation at the sea bottom for different water depths H . The tidal velocity amplitude is $u_0 = 0.04$ m/s, the settling velocity is $w_s = 0.032$ m/s, and the cage width is $b - a = 100$ m.

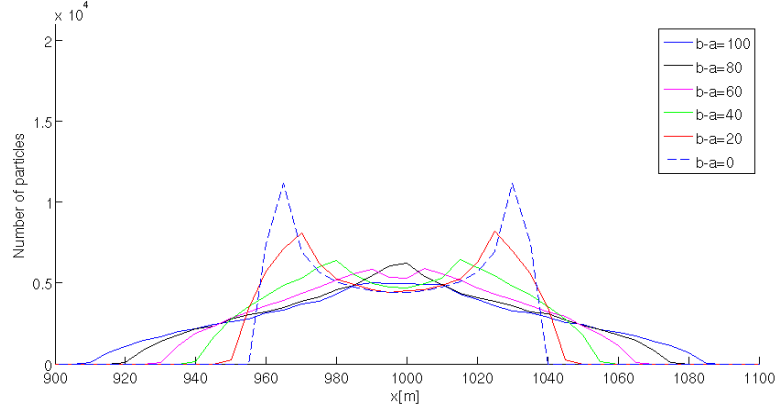


Figure 13: Particles accumulation at the sea bottom for different cage sizes $b - a$. The depth is $H = 100$ m, the settling velocity is $w_s = 0.111$ m/s, the velocity amplitude is $u_0 = 0.04$ m/s, and the maximum disperse distance is $d_{max} = 35.98$ m.

Accordingly, splitting the larger farms into smaller ones, keeping good distance between them will reduce the environmental impacts of the fish waste since less polluted seabed under the fish farm is expected. However, cause must be taken so the d_{max} is larger than half of the cage size.

To summarize these results, if $d_{max}(H, w_s, u_0) < \frac{(b-a)}{2}$, there will be only one maximum concentration point beneath the fish cage centre. If $d_{max}(H, w_s, u_0) > \frac{(b-a)}{2}$, the maximum will split into two maximum concentration points away from the fish cage centre. When the difference $(d_{max}(H, w_s, u_0) - \frac{(b-a)}{2})$ is quite large, the area under the fish cage can be expected to be less impacted by the fish farm since more particles will be transported away from the cage center. If this difference is small, there will still be two maximum concentration points but closer to the cage center.

4 The coupled model in a fjord with one opened boundary

4.1 Model setup

The model domain shown in Figure 14 is the same idealize fjord presented Section 2, but the eastern boundary is closed. At the western boundary the tidal forcing is applied with FRS boundary condition as in Section 2.

The horizontal dimension of the fish cage is 100×100 m, centered at the grid cell at (2000, 600). The particles are released randomly within the cage at 20 m depth. Therefore the falling depth is 80 m which will reduce the sinking time.

4.2 Results

Figure 15 shows the particles accumulations at the bottom computed for different mean settling velocities as variations in particle characteristics are considered. 1.44×10^5 particles are released continuously over 24 hour. The tidal currents amplitude at the cage center is 0.022 m/s.

The results in Figure 15 could be clarified as follows:

1. Particles with mean settling velocity of 0.128 m/s (mean sinking time approximately 10.24 minutes) has one maximum (peak) (solid black line). These particles sink very fast that the influence of the horizontal current is marginal.

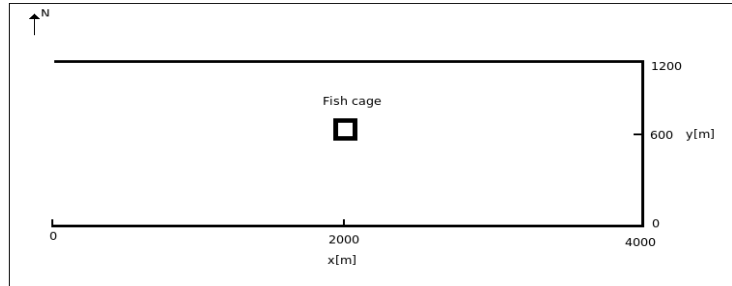


Figure 14: Horizontal configuration of the model domain (Idealized Fjord), with open boundary to the west.

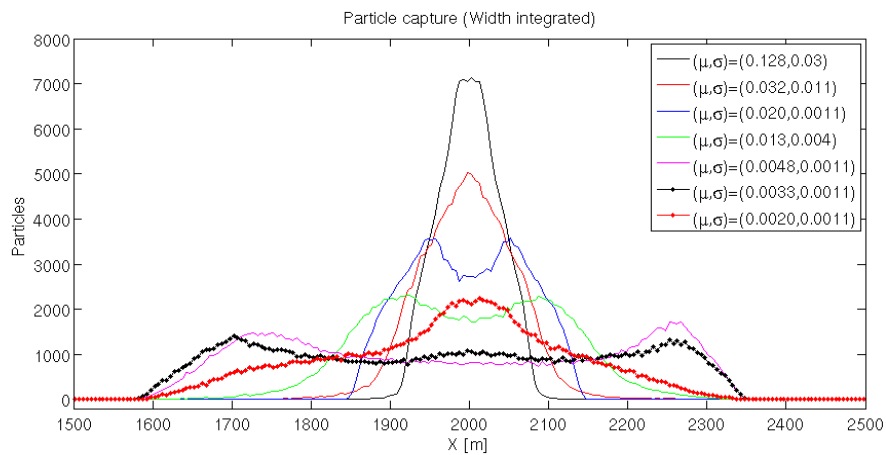


Figure 15: Number of particles settled (width integrated). μ and σ are the mean and standard deviation of the settling velocity, respectively. No consideration for random movement. The tidal velocity amplitude is 0.022 m/s and the cage centre is at $x = 2000$ m, $H = 80$.

2. For particles with mean settling velocities in the range 0.020 to 0.0048 m/s (solid lines), the maximum is split into two peaks away from the cage centre. This splitting is due to the mean sinking time (1.11 to 5.5 hours) approaching $T/2$, which means that most of the particles will spend longer time in the water column. Most of them will therefore be dispersed in one direction and settled before the half of the tidal cycle.
3. For particles with mean settling velocities in the range 0.0033 to 0.002 m/s (dot-solid lines), the two peaks emerge into one peak beneath the cage centre. This is due to the mean sinking time (6.734 to 11.11 hours) approaching the full tidal cycle.

Therefore, particles that has a sinking time that approaches 0 or close to the tidal period T , attain one maximum located under the fish farm. For particles that has sinking times around $T/2$, two maximum peaks in the concentration occurs, one on each side of the fish farm, see Figure 15. Notice that due to the closed boundary to the east the tidal current is weaken, the particles are spreading more far from the cage in towards the opened boundary.

5 Sensitivity to bottom topography

In this section, the coupled model is used to study the sensitivity of particle accumulation due to small variations in bathymetry below the fish cage. A slightly similar study was done by Jusup et al. [2007], where the particle tracking algorithm was forced with current that was extracted from a tidal current record combined with a constant background current (due to wind). In Jusup et al. [2007], no change in the horizontal current due to topographic changes was considered, which is a violation of the continuity equation.

In this work, the idealized fjord setup in Section 4 is used. The reference case is a flat bottom shown in Figure 16(a) is used as reference case. The depth under the cage center is always kept constant in the experiments. The water flux through a vertical section (in y direction) can be computed by

$$U * A_s = \frac{V}{T_v}, \quad (9)$$

where U represents the horizontal current velocity in x direction, A_s is the section area, and T_v denotes the time required to fill a volume V . To raise the surface of a fjord with an amplitude of 0.5 m in 3 hour, the horizontal velocity at a vertical section at the open boundary could be obtained by

$$U = \frac{F_y * F_x * 0.5}{H * S_y * (3 * 3600)}. \quad (10)$$

where F_y , F_x and H are the constant fjord width, length and depth, respectively, and S_y is the width of the section. If the depth under the fish cage is constant, U under the fish cage will also be approximately constant independent on the variations in the bottom topography away from the fish farm.

5.1 Setup

The cage horizontal dimensions are $50 \times 50 \text{ m}^2$. A single settling velocity of (0.0048 m/s) is used. 1.62×10^5 particles were continuously released over 24 hours. The reference setup (flat bottom) is compared with a constant slope bottom, a hill, and a depression beneath the cage.

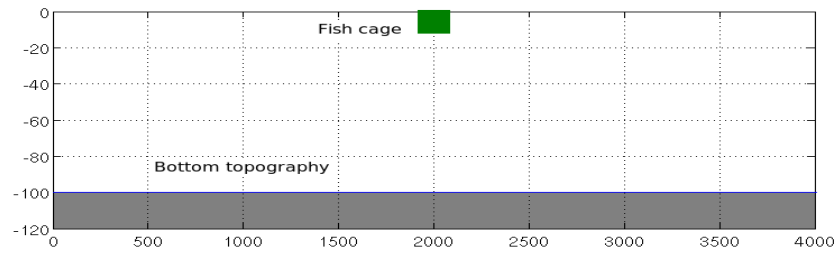
For the flat bottom case, the falling depth for all particles is 75 m, The sinking time is 4.34 hours which means that most particles disperse away from the cage center and they do not return since this sinking time is less than the half of the tidal cycle. The depth under the cage center is 100 m and the initial horizontal positions for the particles are kept constant in all experiments. The bathymetry configurations are shown in Figure 16, where the constant slope equal to 0.04 is shown in Figure 16(b), the 20 m height hill given by

$$H(x, y) = -120 + 20 * e^{-\frac{(x-2000)^2 + (y-600)^2}{200^2}}, \quad (11)$$

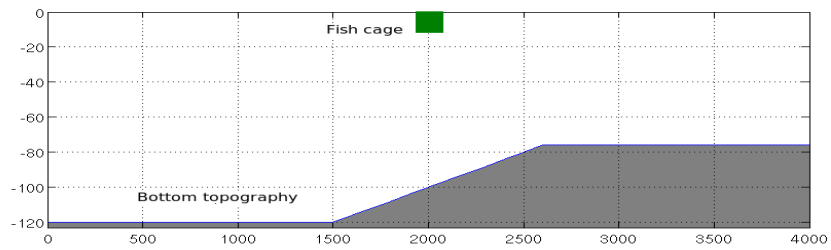
is shown in Figure 16(c), and the 20 m deep depression given by

$$H(x, y) = -80 - 20 * e^{-\frac{(x-2000)^2 + (y-600)^2}{200^2}}, \quad (12)$$

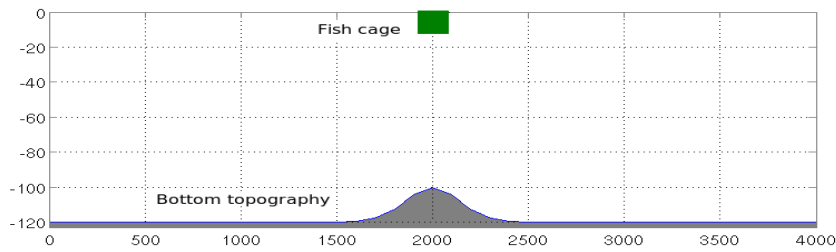
is shown in Figure 16(d).



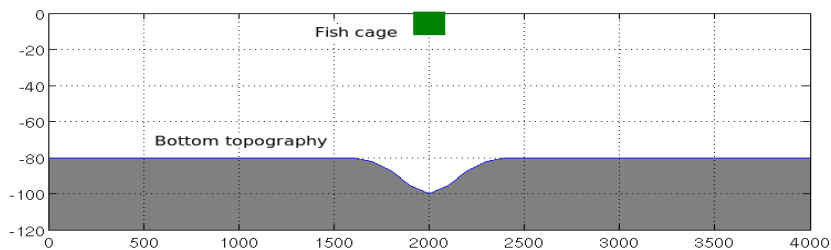
(a) Flat bottom (Reference)



(b) Slope 0.04



(c) 20 m top hill



(d) 20 m deep depression

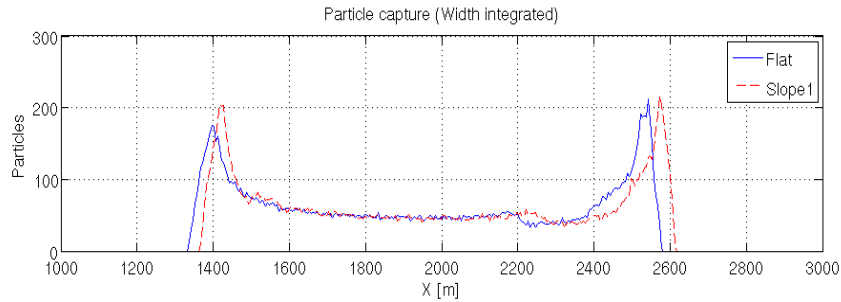
Figure 16: Configuration of a cross-sectional view in the $x-z$ plane of the bottom topographies at $y = 600$ m.

5.2 Results

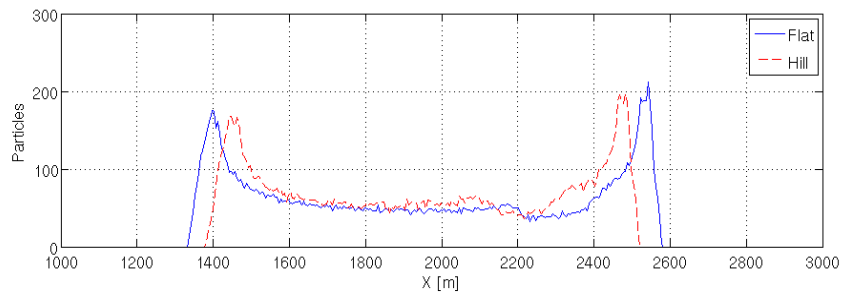
The accumulation of the particles at the bottom (width integrated) compared with the reference case is shown in Figure 17. In general, the slight variations in bottom topography around the cage area has only small affect on the particle distribution and this is due to small variation in the strength of the water flow and the sinking time for the particles.

Figure 17(a) shows that with a slope of 0.04, the particles are spread more towards the closed boundary. The shift to the right in the dispersion curve occurs since the current gets stronger towards the shallower part, even though the sinking time is reduced.

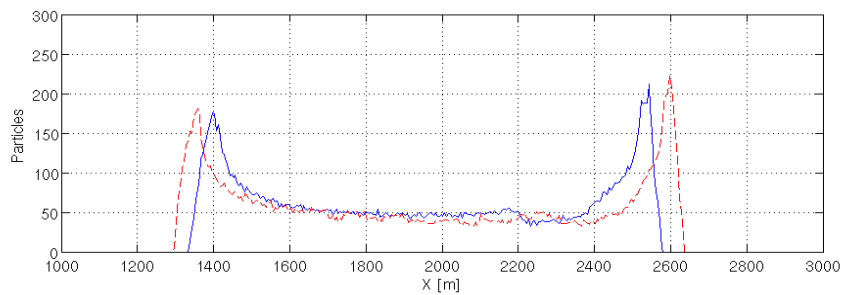
For the 20 m hill, the dispersion is focused closer to the cage center as the horizontal current gets weaker due to the increasing depth around the cage as shown in Figure 17(b). The opposite occurs for the 20 m deep depression as in Figure 17(c), as the depth decreases to 80 m around the depression in Figure 16(d).



(a) flat vs 0.04 slope

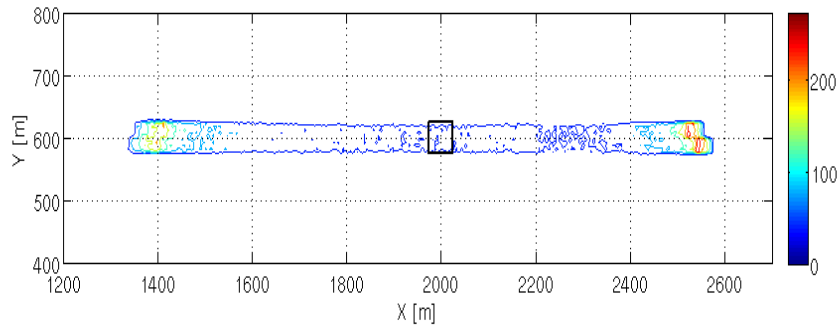


(b) flat vs 20 m top hill

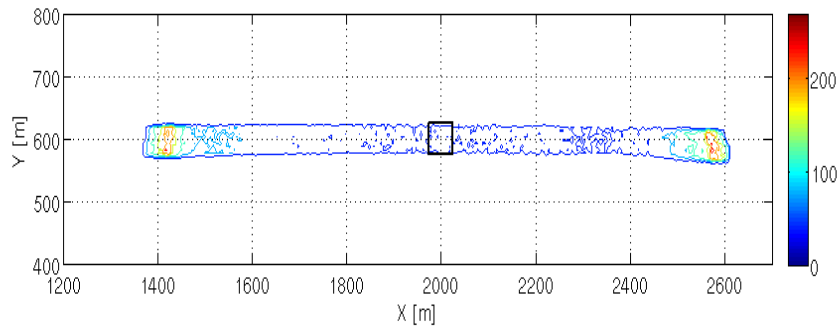


(c) flat vs 20 m deep depression

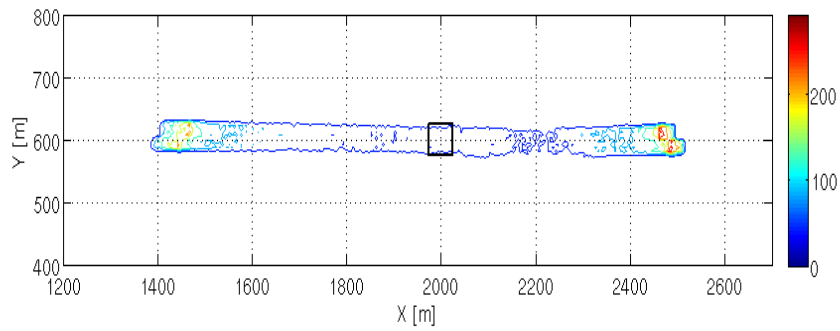
Figure 17: Width integrated Particle accumulation. The settling velocity is 0.0048 m/s and the tidal velocity amplitude at the cage center is 0.041m/s.



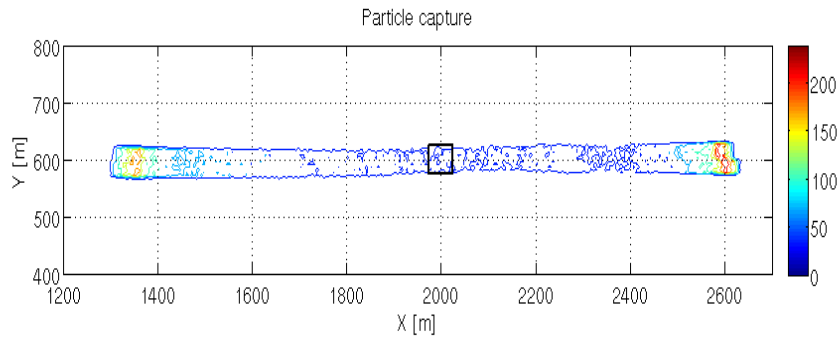
(a) (flat bottom)



(b) 0.04 slope



(c) 20 m top hill



(d) 20 m deep depression

Figure 18: Contour lines of particle distribution for the topographies shown in Figure 16, the settling velocity $\mu = 0.0048$ m/s, the number of the particles is 1.62×10^5 , and the tidal velocity amplitude at the cage center 0.041 m/s.

Figure 18 shows the contour lines of particles distribution for the bottom topographies considered in Figure 16. Notice that the particles accumulation is higher towards the closed boundary which should be expected since the horizontal velocity is weaker. see Figure 19. For areas where the tidal current is quite weak or the settling velocity is quite large, differences in the particle footprint due to smaller variations in bathymetry are small such as in Figure 20 and can be neglected.

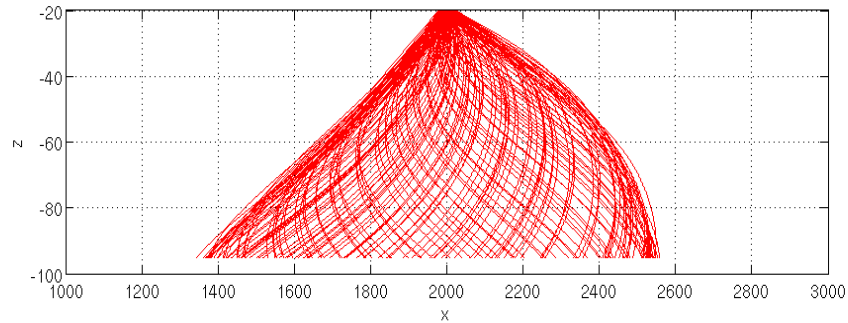
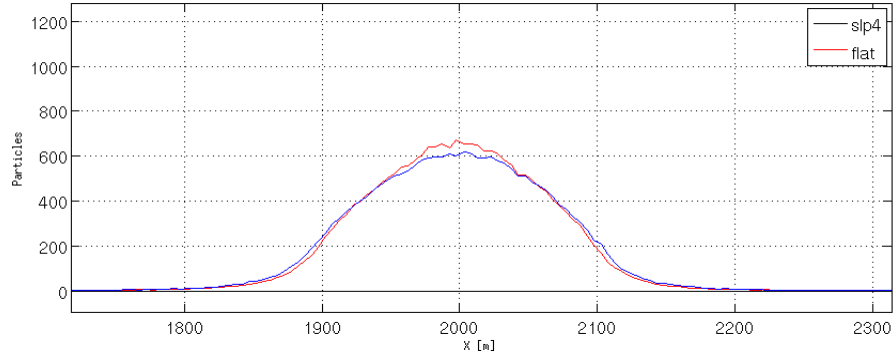
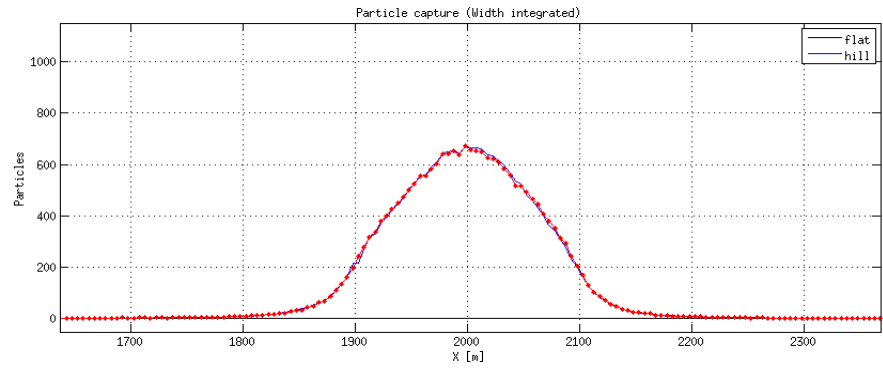


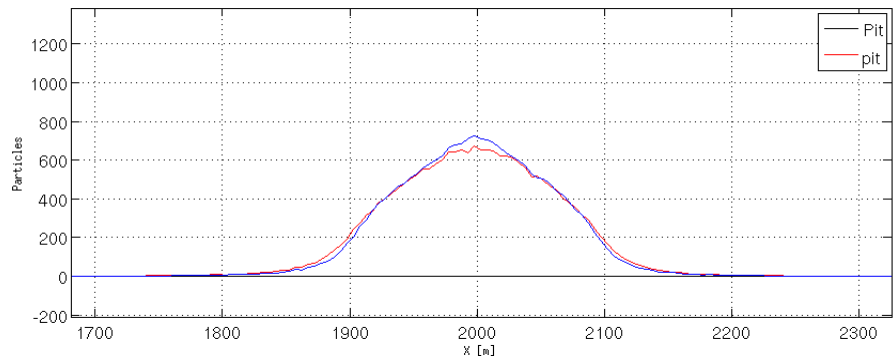
Figure 19: Pathes of particles, mean settling velocity $\mu = 0.0048$ m/s with 0 standard deviation, the tidal velocity amplitude at the cage center 0.041 m/s.



(a) Particles hit the bottom: flat vs slope



(b) Particles hit the bottom: flat vs Hill



(c) Particles hit the bottom: flat vs Pit

Figure 20: Settling velocity $\mu = 0.032 \text{ m/s}$ $\sigma = 0.011 \text{ m/s}$, the number of particles is 2.16×10^5 , and $T = 3 \text{ days}$. The tidal amplitude $u_0 = 0.021 \text{ m/s}$ at the cage center.

6 Summary

Three dimensional particle tracking model is coupled to BOM and tested in an idealized fjord with a tidal currents forcing. The results of particle accumulations over the bottom were in very good agreement with the results generated by an analytical model. The maximum concentration rate of waste under the fish cage can split into two maximum areas outside the cage area depending on the tidal currents, fjord depth and the settling velocity. If the sinking time is close to a full tidal period, the particles will end up under the fish cage. This also occurs for the very fast sinking particles (heavy particles).

The study shows also that increasing the cage size increases the likelihood for food and faecal pellets to end up beneath the fish cage which can make the local pollution more severe than the case for smaller fish cages. This might be against the interests of the fish farming industry which is often interested in increasing the production (biomass) by introducing larger fish cages.

Through this study, the performance of the Coupled Model has been investigated and verified. The model system will now be applied in more realistic studies to improve our understanding of dispersal from fish farms where factors like variations in bottom topography, stratification, and forcing (wind, river runoff) are present. Further model studies may be used to help selecting sites for the fish farms to ensure a sustainable and environmentally friendly fish farm production.

The blocking effects of the fish cage and velocities generated by the fishes movement inside the cage can change the free flow in and near the fish cage. These effects can introduce fluid velocities that can influence the sinking velocity of the particulate matter and affect the spreading and plume generation of the dissolved waste. Further, sediment resuspensions in areas where the near bed flow is of significant strength will affect the particle distribution at the seabed. These effects are outside the scope of this work, but should be considered in up following studies.

Acknowledgment

This research has received support from The Research Council of Norway through NFR 146526/420: ECORAIS.

References

- H. Berntsen, Z. Kowalik, S. Sælid, and K. Sørli. Efficient numerical simulation of ocean dynamics by splitting procedure. *Model. Ident. Control*, 2:181–199, 1981. 2.1
- J. Berntsen, J. Xing, and G. Alendal. Assessment of non-hydrostatic ocean models using laboratory scale problems. *Cont. Shelf Res.*, 26:1433–1447, 2006. 2.1
- Y. S. Chen, M. Beveridge, and T. C. Telfer. Settling rate characteristics and nutrient content of the faeces of Atlantic salmon (*Salmo salar* L.) and the implications for modelling of solid wastes dispersion. *Aquaculture Res.*, 30:395–398, 1999. 2.2.1
- C. Cromey, T. Nickell, and K. Black. Depomod-modelling the dispersion and biological effects of waste solids from marine cage farms. *Aquaculture*, 214:211–139, 2002. 1, 2.2.1
- A.M. Doglioli, M.G. Magaldi, L. Vezzulli, and S. Tucci. Development of a numerical model to study the dispersion of wastes coming from a marine fish farm in the ligurian sea (western mediterranean). *Aquaculture*, 231:215–235, 2004. 1

- R. Dudley, V. Panchan, and C. Newell. Application of a comprehensive modeling strategy for the management of net-pen aquaculture waste transport. *Aquaculture*, 187:319–349, 2000. 1
- M. Jusup, S. Gecek, and T. Legovic. Impact of aquaculture on the marine ecosystem: Modelling benthic carbon loading over variable depth. *Ecol. Model.*, 200:459–466, 2007. 1, 5
- Z. Kowalik and T. S. Murty. *Numerical Modeling of Ocean Dynamics*. Advanced Series on Ocean Engineering Vol. 5. World Scientific, 1993. 2.1
- S. H. Magill, H. Thetmeyer, and C. J. Cromy. Settling velocity of faecal pellets of gilthead sea bream (*Sparus aurata*) and sea bass (*Dicentrarchus labrax* L.) and sensitivity analysis using measured data in a deposition model. *Aquaculture*, 251:295–305, 2006. 2.2.1
- E. A. Martinsen and H. Engedahl. Implementation and testing of a lateral boundary scheme as an open boundary condition for a barotropic model. *Coast. Eng.*, 11:603–637, 1987. 2.1
- V. Panchang, G. Cheng, and C. Newell. Modeling hydrodynamics and aquaculture waste transport in coastal Maine. *Estuaries*, 20:14–41, 1997. 1
- W. Silvert and J. W. Sowles. Modelling environmental impacts of marine finfish aquaculture. *J. Appl. Ichtyol.*, 12:75–81, 1996. 1
- Ø. Thiem, J. Berntsen, K. Selvikvåg, and J.H. Fosså. Numerical study of particle encounters with an idealized coral reef with focus on grid resolutions and viscosities. Tech. rep., Bergen center for computational science, Uni BCCS, 2008. 2.2